

RESEARCH

Open Access



Comparative transcriptional analysis and identification of hub genes associated with wing differentiation of male in *Aphis gossypii*

HUANGFU Ningbo^{1,2}, SHI Qingyu¹, CHEN Lulu³, MA Xiaoyan^{1,2*}, ZHANG Kaixin¹, LI Dongyang¹, WANG Li¹, ZHU Xiangzhen¹, JI Jichao^{1,2*}, LUO Junyu^{1,2} and CUI Jinjie^{1,2}

Abstract

Background: *Aphis gossypii* Glover (Hemiptera: Aphididae), a worldwide polyphagous phloem-feeding agricultural pest, has three wing morphs (winged parthenogenetic female, gynopara, and male) in the life cycle. The exclusive males could fly from summer hosts to winter hosts, which are essential for gene exchanges of cotton aphid populations from different hosts or regions. However, the molecular mechanism of wing differentiation of male in *A. gossypii* remains unclear.

Results: Morphological observation of male *A. gossypii* showed that there is no distinct difference in the external morphologies of the 1st and 2nd instar nymphs. The obvious differentiation of wing buds started in the 3rd instar nymph and was visible via naked eyes in the 4th instar nymphal stage, then adult male emerged with full wings. According to morphological dynamic changes, the development of wings in males were divided into four stages: preliminary stage (the 1st instar to 2nd instar), prophase (the 3rd instar), metaphase (the 4th instar), anaphase (the 5th instar). Results of feeding behavior monitoring via EPG (electrical penetration graph) technology indicated that although the male cotton aphids had strong desire to feed (longer duration of C 55.24%, F 5.05% and Pd waves 2.56%), its feeding efficiency to summer host cotton was low (shorter E1 3.56% and E2 waves 2.63%). Dynamic transcriptome analysis of male aphid at 5 different developmental periods showed that in the 3rd instar nymph, the number of up-regulated DEGs was significant increased, and time-course gene transcriptional pattern analyses results also showed that numerous genes categorized in clusters 3, 5, and 8 had the highest expressed levels, which were consistent with morphological changes of wing buds. These results indicate that the 3rd instar nymph is the critical stage of wing bud differentiation in males. Furthermore, through pathway enrichment analysis of DEGs and WGCNA, it revealed that the neuroactive ligand-receptor interaction, Ras signaling pathway, dopaminergic synapse, circadian entrainment and the corresponding hub genes of *PLK1*, *BUB1*, *SMC2*, *TUBG*, *ASPM*, the kinesin family members (*KIF23*, *KIF20*, *KIF18-19*) and the novel subfamily of serine/threonine (Aurora kinase A and Aurora kinase B) probably played an important role in the critical stage of wing bud differentiation.

*Correspondence: maxy_caas@126.com; hnnydxjc@163.com

¹ Zhengzhou Research Base, State Key Laboratory of Cotton Biology, Zhengzhou University, Zhengzhou 450001, China
Full list of author information is available at the end of the article



© The Author(s) 2022. **Open Access** This article is licensed under a Creative Commons Attribution 4.0 International License, which permits use, sharing, adaptation, distribution and reproduction in any medium or format, as long as you give appropriate credit to the original author(s) and the source, provide a link to the Creative Commons licence, and indicate if changes were made. The images or other third party material in this article are included in the article's Creative Commons licence, unless indicated otherwise in a credit line to the material. If material is not included in the article's Creative Commons licence and your intended use is not permitted by statutory regulation or exceeds the permitted use, you will need to obtain permission directly from the copyright holder. To view a copy of this licence, visit <http://creativecommons.org/licenses/by/4.0/>.

Conclusion: This study explored morphological changes and genes transcriptional dynamics males in cotton aphid, revealed the phenomenon of low feeding efficiency of winged males on summer host cotton, and identified key signaling pathways and potential hub genes potentially involved in wing bud differentiation of male in *A. gossypii*.

Keywords: *Aphis gossypii*, EPG, Wing bud differentiation, Dynamic transcriptome, WGCNA

Background

Aphis gossypii Glover (Hemiptera: Aphididae), a world-wide agricultural pest with extremely complex life history, distributed in more than 171 countries and feeding on 65 plant genera, causes huge losses to crop yield and quality every year (Willis 2017). In recent decades, excessive use of chemical pesticides, over large-area cultivation of Bt cotton and global warming have led to continual outbreak of piercing-sucking pests especially *A. gossypii* in China (Chen et al. 2013; Lu et al. 2010; Sun et al. 2015). The damage spread of cotton aphid was closely related to three winged morphs, in which winged male was indispensable for life cycle (Ji et al. 2021). In northern China, *A. gossypii* differentiates into winged males, then flies to winter hosts to mate with sexual females which lays fertilized overwintering eggs in autumn. The wing formation of male promotes gene exchanges of colonies from different geographical regions and hosts, which is crucial for the survival and reproduction of *A. gossypii* (Kwon et al. 2017). Considerable attempts have been made to successfully induce male *A. gossypii* under low temperature and short light conditions (Ji et al. 2021). However, the dynamic morphological characteristics, the development process, the feeding behavior, and particularly the molecular mechanism of wing differentiation in male *A. gossypii* remains enigmas.

The regulation mechanism of male wing differentiation was well studied in pea aphid *Acyrtosiphum pisum*, in which the sex-linked locus on the X-chromosome named *aphicarus* determines the wing production of male (Braendle et al. 2005; Ogawa et al. 2013). That is, male wing polymorphism exists in *A. pisum* and is under the control of exclusively genetics. However, the differentiation of wings in male *A. gossypii* was quite different: all males had wings (Lee et al. 2015). Both males of *A. pisum* and *A. gossypii* had only one X-chromosome, but their wing differentiation patterns were obviously distinct, which were related to the biological characteristics of these two species: *A. pisum* was monophagous and no-host-alternating, whereas *A. gossypii* was polyphagous and host-alternating. Long-distance flights were not fully essential for the former in autumn, hence wings in males of *A. pisum* were alternative. In contrast, males are exclusively winged to migrate between primary host (usually woody) and the second host (usually herbaceous) in the latter (Ardie et al. 2017). Moreover, only 12 species

belong to the no-host-alternating category own male wing polymorphism, which account for less than 2% of the recorded aphid species (Blackman et al. 2007). Therefore, the differentiation of male wings of cotton aphid is more representative in Aphididae to some extent. Studies on male wing differentiation of cotton aphid will benefit for understanding male wing production in host-alternating aphids and developing genetic control strategies against this pest through the disruption of male migratory.

Studies on aphid wing differentiation also have focused on parthenogenetic aphid. The generation of winged morph is mainly influenced by environmental factors such as crowding, photoperiod, nutrition and natural enemies, which is called non-genetic polymorphism. Traditional histological methods were widely used to explore wing differentiation in parthenogenetic aphid (Shull 1938; Johnson et al. 1960; Ganassi et al. 2005a, b). Histological observation results showed that the development of wing is inherent, whether or not they eventually develop into winged form, whereas wingless morphology is achieved by altering the original developmental pathway in the embryonic or nymphal stage (Braendle et al. 2006). The endogenous factors that regulate the wing differentiation of parthenogenetic aphid include ecdysone, octopamine, and insulin. Activation or inhibition of these three signaling pathways can affect the percentage of winged aphid separately (Wang et al. 2016; Ding et al. 2017). In contrast, although the generation of male *A. gossypii* can be induced by low temperature, crowding and short photoperiod, the corresponding process of wing bud differentiation is still not clear.

In the study, we manually counted and analyzed the distribution of wingless or wing male in recorded aphids derived from literatures firstly. Then, the morphological changes of male *A. gossypii* at different developmental stages were systematically observed and feeding behavior of males were monitored via electrical penetration graph technology (EPG). Subsequently, gene expression patterns clustering, differential expressed genes (DEGs) identification, KEGG enrichment, and weighted correlation network analysis were integrated to explore pivotal genes and signal pathways potentially involved in the regulation of wing differentiation in male of cotton aphid. Taken together, this study forms a basis for deciphering the molecular mechanisms underlying wing production

of males in the cotton aphid and also provides valuable resources for future studies on male wing formation in host-alternating aphid species.

Materials and methods

Investigation of male aphid wing in Aphididae

The aphid species in which males were observed in field were counted from the book of *Aphids on the World's Herbaceous Plants and Shrubs* through keywords searching (Blackman et al. 2007). The retrieval results were listed in MS Excel and categorized manually at subfamilies, races, and genera levels, respectively.

Male induction and morphological observation

Aphis gossypii colony, collected originally in Anyang, China, was reared on cotton seedlings under controlled laboratory conditions for more than 50 generations before the start of all experiments ($25 \pm 1^\circ\text{C}$, 75% relative humidity, 16L: 8D photoperiod). Males were induced by rearing newly-born viviparous nymphs (the first generation, G_1) at short day (SD) conditions as our previous methods (Ji et al. 2021). Offspring (the second generation, G_2) produced by G_1 mothers about 8 days later will develop into males. The duration time of each nymph stage and adult longevity were calculated with more than 20 males. The body morphology of male at different developmental stages and adult male testes were visualized using a SteREO Discovery V8 microscope (Zeiss, Germany), in which the testes were isolated in phosphate-buffered saline (PBS) buffer. In addition, the body and antennae lengths as well as head widths in each of male developmental stage were measured with more than 30 males.

Males feeding monitoring via electrical penetration graph recording

Electrical penetration graph (EPG) apparatus (DC-EPG Giga-8, Wageningen, Netherlands), placed in Faraday metal shield, were used to monitor the feeding behavior of male *A. gossypii* on cotton (CCRI 49) seedlings. The experiments were according to a previously described protocol with some improvements as follows (Elisa et al. 2016). New molting adult males were connected to the flexible gold wires (10 μm diameter \times 4 cm length) through their dorsal thorax with the water-soluble conductive silver glue. After staved for one hour, each individual was placed on a leaf of cotton seedling at four-leaf stage. The EPG signal of each male was monitored continuously for 12 h via software Style + d, and the waveforms were analyzed by using software style + a. During the 12-h recording, six waveforms described by Tjallingii (1988) and Prado and Tjallingii (1994), were identified as follows: (1) Np (non-penetration) waveform appears

due to stylet withdrawal; (2) waveform C (the probing period waveform consists of aphid mouth needles probing between mesophyll cells or outside the sieve molecules in phloem); (3) Pd waveform (potential drops, the aphid's mouth needles probe inside the living cells); (4) F waveform (the aphid mouth needles encounter mechanical resistance outside the plant tissues and cells); (5) E1 waveform (the aphids' mouth needles secrete saliva into the sieve elements); (6) E2 waveform (the aphid mouth needles feed passively within the screen tube). EPG variables were processed and calculated using EPG-Excel data workbook (Sarria et al. 2009). A total of 12 replicates were set with each male.

Sample preparation for RNA-seq

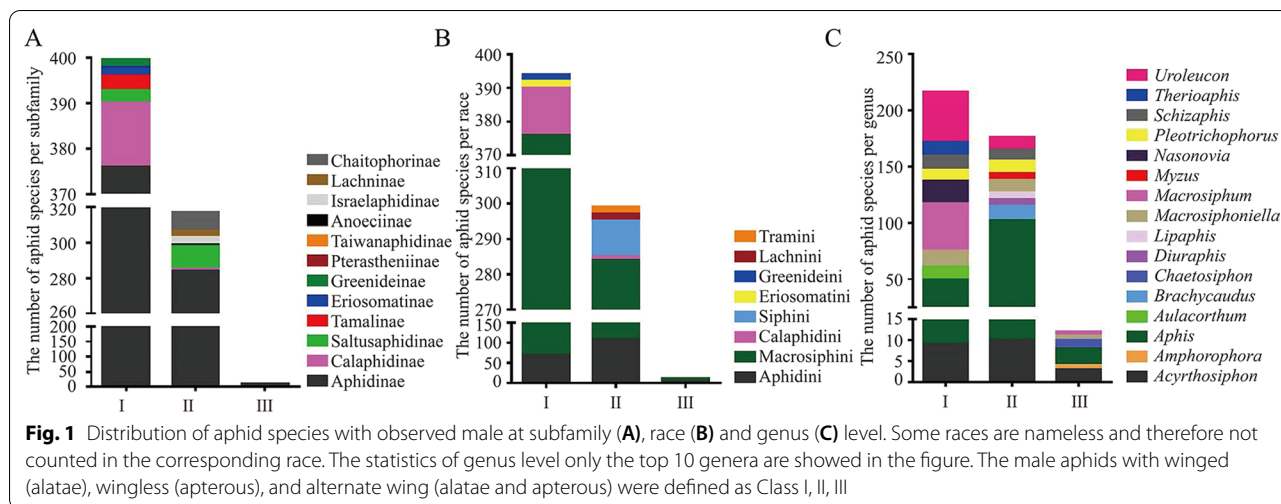
Whole bodies of males at different developmental stages including the 1st to the 4th instar nymphs and adults were collected, respectively. Total RNA of males in each developmental stage was extracted separately using TRIzol[®] reagent (Promega, USA) following the manual. The RNA concentration was assessed by a spectrophotometer Nanodrop 2000 (Thermo, USA), and the RNA quality was assessed using Agilent 2100. Synthesis of cDNA and Illumina library generation were completed at Beijing Genomics Institute (BGI) (Shenzhen, China) using BGISEQ-500 sequencing. There were three biological replicates for each development stage of males, and each biological replicate contained 100 males, respectively.

Transcriptome assembly and gene annotation

After sequencing, the raw reads were obtained and subsequently the adapter sequences and low-quality reads were filtered to acquire clean reads. The RNA-seq clean reads were aligned to the *A. gossypii* genome (Quan et al. 2019) using HISAT2 (Kim et al. 2015). Transcripts of each sample were reconstructed using StringTie and the new transcripts were identified using Cufflinks (Pertea et al. 2015; Trapnell et al. 2012). Those new protein-coding transcripts were predicted by CPC and aligned to protein databases, including Nr, KEGG by blastx with the cutoff E-value of $10\text{E}-5$ (Altschul et al. 1990).

Differentially expressed genes identification

Gene expression levels in each library were calculated by fragments per kilobase per million reads (FPKM) method using Bowtie2 and RESM (Langmead et al. 2012; Dewey and Li 2011). Fold change (FC), the relative expression level of a gene in one stage to another, and *P*-value adjusted in multiple tests by false discovery rate (FDR), were used to determine the differentially expressed genes between two stages by DEseq2 (Love et al. 2014; Reiner et al. 2003). Ultimately, $\text{FC} > 2$ and adjusted $P < 0.001$ were the thresholds to determine significant differences



in gene expression. All raw RNA-Seq read data are deposited in the NCBI Short Read Archive under the BioProject accession code PRJNA807005. The expression profiles were assigned to 9 clusters by using the fuzzy *c*-means algorithm implemented in the R package Mfuzz (v2.34.0, -c 9 -m 1.25) (Lokesh et al. 2007). Significantly enriched KEGG pathways were identified through hypergeometric tests at the criteria of $P < 0.05$ by function *phyper* (<https://search.r-project.org/CRAN/refmans/DPQ/html/phyper.html>). Pearson correlation coefficients of all gene expression level between each two samples were calculated by function *cor* and reflected in the form of heat maps (<https://cran.r-project.org/web/packages/corrplot/vignettes/corrplot-intro.html>). *Princomp* was used for PCA analysis (<https://search.r-project.org/CRAN/refmans/ggfortify/html/fortify.pcomp.html>).

Gene co-expression network construction and visualization

WGCNA as a typical algorithm is widely used in gene co-expression network identification (Horvath et al. 2008). We constructed Weighted Gene Co-expression Network by the WGCNA package in R software (Langfelder et al. 2008). The R package and its source code and additional material is freely available at <https://horvath.genetics.ucla.edu/html/CoexpressionNetwork/Rpackages/WGCNA/>. The experimental procedures referred to the previous method (Zhang et al. 2021). The resulting modules were represented and visualised using Cytoscape_v3.8.0 (<http://www.cytoscape.org/>).

qRT-PCR for validation of RNA-seq data

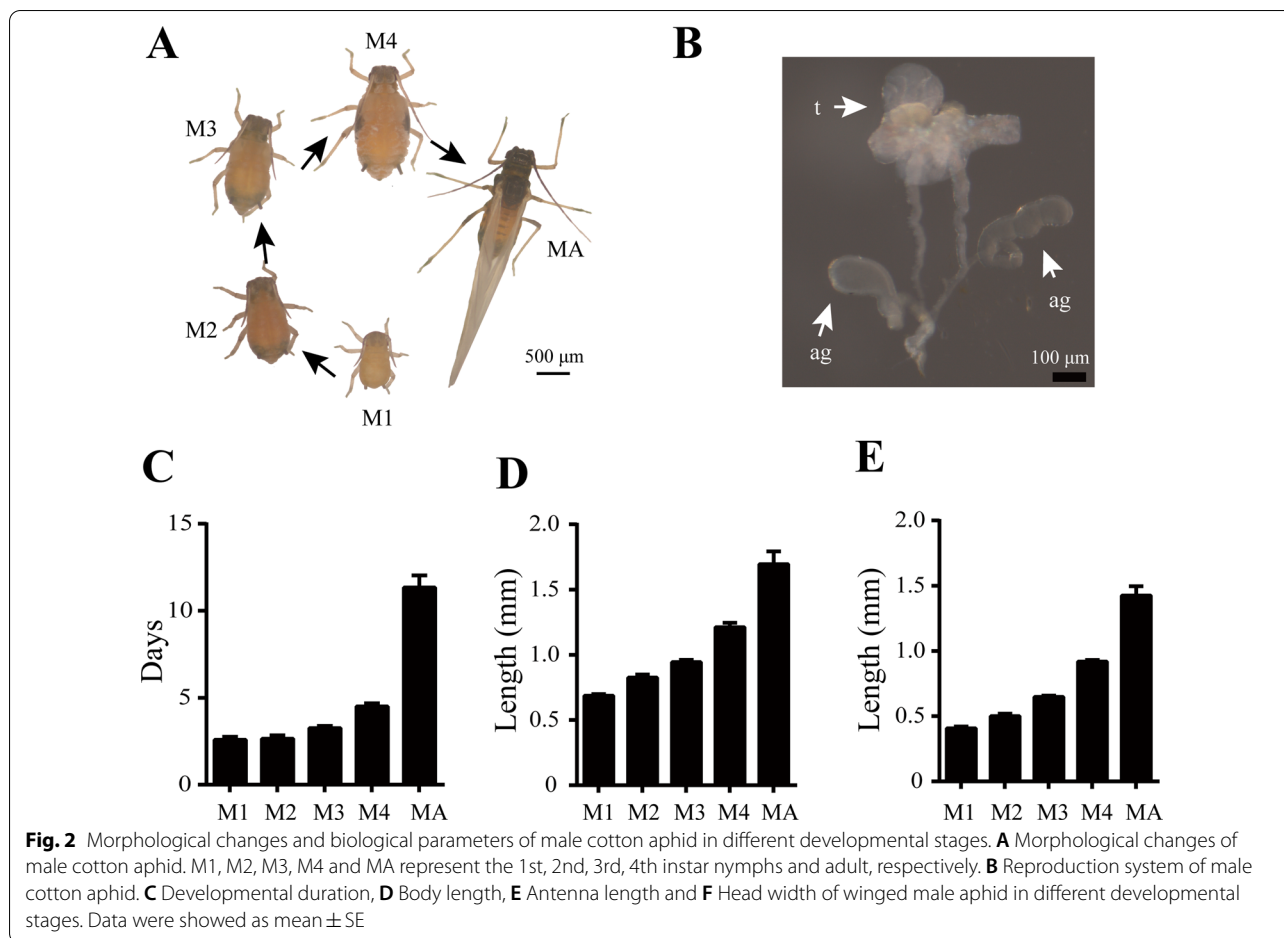
The relative expression of genes was quantified by qRT-PCR utilizing a Light Cycler 480 machine (Roche Diagnostics, Switzerland). The reactions included 2 μL cDNA

template, 7.2 μL nuclease-free water, and 0.4 μL primer F/R. qRT-PCR procedure was set as follows: 94 °C for 30 s, 45 cycles of 94 °C for 5 s, 55 °C for 15 s, and 72 °C for 10 s. Melting curve was conducted to verify the specificity of amplification. Gene-specific primers were designed with Primer Premier 6 and *GAPDH* gene was used as the internal control to normalize expression level (Gao et al. 2017). All primers are listed in Additional file 1: Table S1. The relative expression level of each gene was calculated by the $2^{-\Delta\Delta Ct}$ method (Livak et al. 2001). Three biological replicates were assayed for statistical analysis.

Results

Outline of male wing morph in Aphididae and cotton aphid

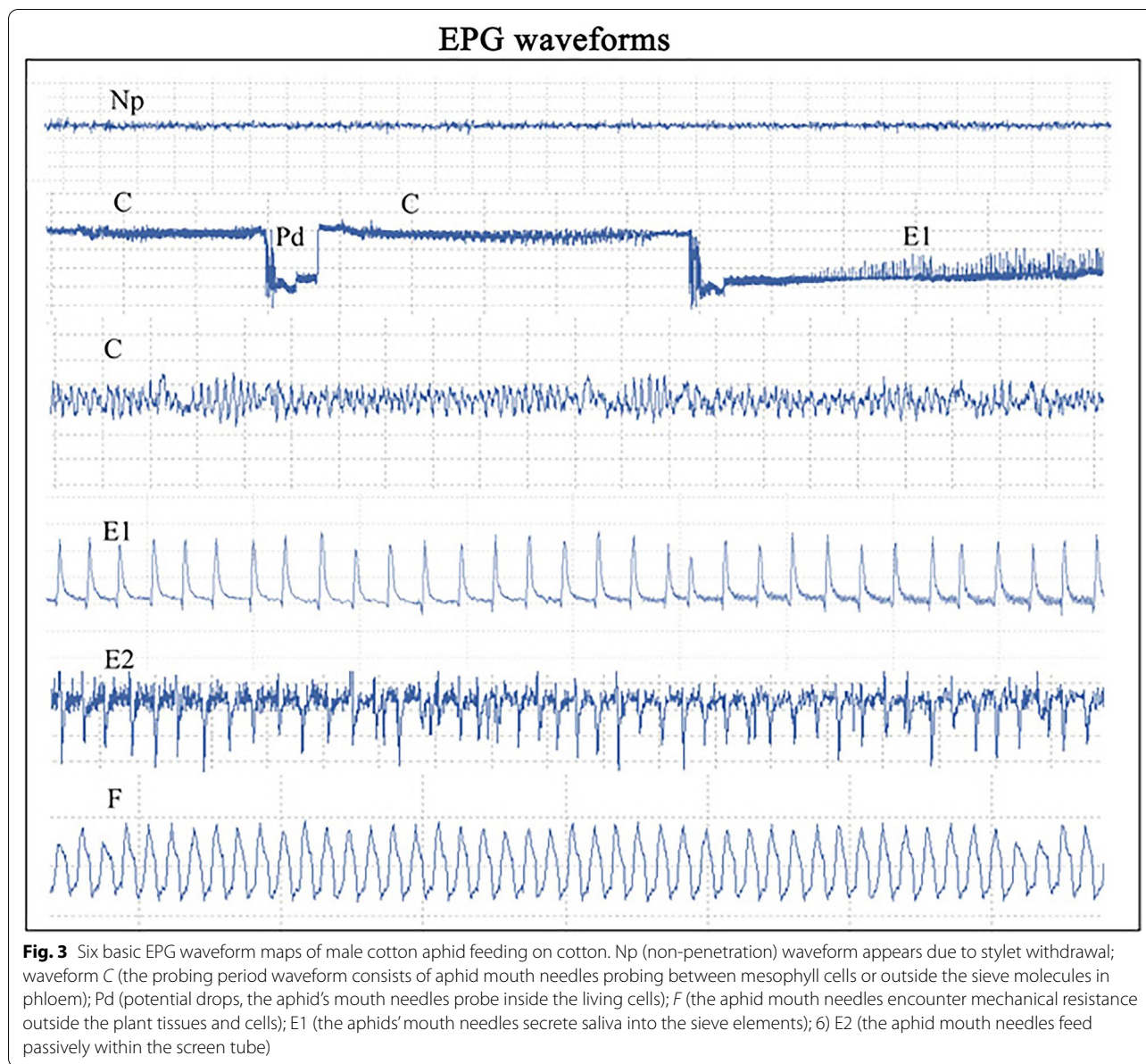
Male aphids were observed in 731 species of Aphididae, which belong to 12 subfamilies, 8 races, 153 genera (Additional file 2: Table S2). At the subfamily level, male aphids were recorded mainly in Aphidinae (672), Saltusaphidinae (16), and Calaphidinae (15) (Fig. 1A). At the race level, male aphids were observed primarily in Macrosiphini (490) and Aphidini (183) (Fig. 1B). At the genera level, male aphids were mostly found in *Aphis* genus (137), followed by genera *Uroleucon* (56) and *Macrosiphum* (48) (Fig. 1C). Furthermore, males were exclusively alate in 402 species, exclusively apterous in 317 species, and alternative wing (alate or apterous) in 12 species. We defined these three aphid species as Class I, II, III, in which males were winged, wingless, alternate wing, respectively (Fig. 1, Additional file 2: Table S2). At the subfamily level, aphids in Tamaliinae (3), Eriosomatinae (2), Greenideinae (2), Pterastheniinae (1), and Taiwanaphidinae (1) belonged to Class I, those in Chaitophorinae (10), Israelaphidinae (4), Lachninae (4), Anoeciinae (1) belonged to Class II. Emphatically, 376,



284, 12 species in Aphidinae belonged to Class I, II, III, respectively (Fig. 1A). At the race level, aphids in Eriosomatini (2) and Greenideini (2) belonged to Class I, those in Siphini (10), Lachnini (2), Tramini (2) belonged to Class II. Specifically, 69, 109, 4 species in Aphidini and 307, 175, 8 in Macrosiphini belonged to Class I, II, III, respectively (Fig. 1B). At the genus level, aphids in Therioaphis (12) and Diuraphis (6) belonged to Class I and II, respectively; 136 and 72 species scattered in 11genera were categorized into Class I, II, respectively; 114, 121, 12 species in 6 genera were classified into Class I, II, III, respectively (Fig. 1C). Obviously, males in families of Taiwanaphidinae, Eriosomatinae, Greenideinae, Pterastheniinae, and Tamaliinae subfamilies were all winged, and those in Anoeciinae, Israelaphidinae, Lachninae, and Chaitophorinae subfamilies were all wingless. At the genera level, all males are wingless mainly in *Therioaphis* and *Rhopalomyzus*, and all males are winged mainly in *Diuraphis*, *Lipaphis* and *Thripsaphis*.

Morphological changes especially wing bud differentiation and reproductive organ of males were showed in

Fig. 2A, 2B. No distinct difference in the external morphologies between the first- and second-instar male nymphs were observed. The presumptive wing bud apophyses were visible on both sides of the second- and third-thoracic sections in the 3rd instar nymph and can be observed clearly by naked eyes in the 4th instar nymph. Adult male emerged with full wings, sclerotized and hardening thorax, as well as black streaks on the yellow abdomen. Taken together, wing differentiation in male of cotton aphid can be divided into four stages: preliminary stage (the 1st instar to 2nd instar), prophase (the 3rd instar), metaphase (the 4th instar), anaphase (the 5th instar). Besides, the duration time of the 1st, 2nd, 3rd, 4th instar nymphs of male is 2.59 d, 2.65 d, 3.26 d, 4.5 d, respectively, and the longevity of male adult is 11.33 d (Fig. 2C). The body length of the first-, second-, third-, fourth-instar nymphs and adult were 0.69, 0.83, 0.94, 1.21, 1.67 mm, respectively (Fig. 2D), the corresponding antenna length were 0.41, 0.50, 0.65, 0.92, 1.43 mm, respectively (Fig. 2E), and the head width were 0.20, 0.22, 0.24, 0.25, 0.37 mm, respectively (Fig. 2F). Generally, the duration times, body length, antenna length and head

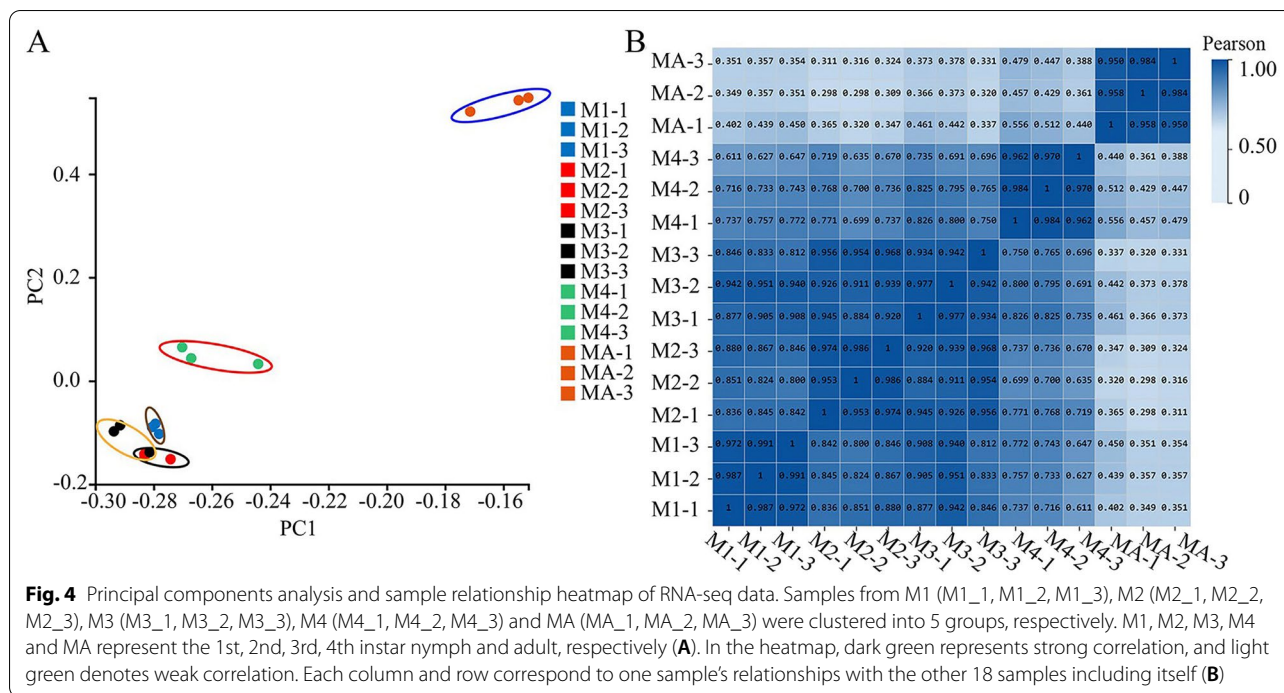


width of male increases slowly from the 1st to 4th instar nymphs until the significant differences were observed in the 3rd, 4th instar nymph and adult (Fig. 2 and Additional file 3: Table S3).

Male *A. gossypii* feeding behavior monitoring via EPG
 Males feeding on cotton seedlings showed typical feeding behavior patterns that have been previously documented with 6 clear probe events followed successively by Np

Table 1 The statistics analysis of EPG parameters

EPG parameters	Np	C	Pd	F	E1	E2
<i>Statistical analysis</i>						
The number of waves	33.07 ± 6.22	53.71 ± 9.96	242.64 ± 29.24	13.21 ± 4.90	14.21 ± 2.94	6.29 ± 2.00
Mean duration /s	1100.54 ± 462.25	488.34 ± 88.36	112.65 ± 101.23	443.80 ± 164.79	166.65 ± 61.95	190.58 ± 57.96
Total duration /min	231.93 ± 29.86	397.76 ± 37.16	18.41 ± 2.46	36.37 ± 10.08	25.66 ± 5.15	18.96 ± 4.74
The percentage of total duration /%	32.21 ± 4.15%	55.24 ± 5.16%	2.56 ± 0.34%	5.05 ± 1.40%	3.56 ± 0.72%	2.63 ± 0.66%



waveform, C waveform, Pd waveform, E1 waveform, E2 waveform, F waveform, respectively (Fig. 3). Feeding behavior parameters of male cotton aphids are showed in Table 1. In 12 h, the average frequency of probing, duration time and the average duration of each wave pattern of male cotton aphids on summer host cotton were significantly different. Pd waveform contains the most probing numbers (242.64), followed by waveform of C, Np, E1, F, E2, with the numbers of 53.71, 33.07, 14.21, 13.21, 6.29, respectively. The longest total duration time was C waveform (397.76 min, 55.24%), which was much higher than waveform of Np (231.93 min, 32.21%), F (36.37 min, 5.05%), E1 (25.66 min, 3.56%), E2 (18.96 min, 2.63%) and Pd (18.41 min, 2.56%). Furthermore, the mean duration times are in order as follows: Np (1 100.54 s), C (488.34 s), F (443.80 s), E2 (190.58 s), E1 (166.65 s), Pd (112.65 s). Obviously, the mean duration times of probing waves (C waveform, F waveform, Pd waveform) was much longer than those of feeding waves (E1 waveform and E2 waveform).

Time-course transcriptome profiling of male *A. gossypii*

RNA sequencing was performed to monitor the transcriptomic dynamics across of male cotton aphid development process. A total of 918. 37 M clean reads were obtained with an average Q30 percentage of 88.41% from 12 nymphal and 3 adult samples, in which the mean genome and gene set mapping percentage of clean reads were 87.74% and 78.63%, respectively (Additional file 4:

Table S4). Principal components analysis (PCA) and Pearson correlation coefficient analysis showed that the samples during different developmental stages exhibited significant separation, whereas the variability was low between different replicates in the same stage (Fig. 4A and 4B). Specifically, the Pearson correlation coefficient of intra-group gene expression levels in each stage was all greater than 0.9, which indicated that our RNA-seq datas were reliable for further analysis.

Clustering gene time course expression of male was implemented by Fuzzy c-means algorithm through Mfuzz software. 11 936 genes involved in male cotton aphid development were divided into 9 distinct clusters of temporal patterns which representing different expression kinetics (Fig. 5 and Additional file 5: Table S5). Among these, cluster 8 includes the maximum gene number of 1 732, followed by cluster 3 (1 674), cluster 7 (1 566), cluster 4 (1 519), cluster 2 (1 301), cluster 5 (1 295), cluster 1 (994), cluster 9 (961), cluster 6 (894). Moreover, genes in cluster 2 were upregulated as a whole in male development, and genes in cluster 4 and 7 were downregulated mostly, whereas those in cluster 1, 3, 5, 6, 8, and 9 displaying a bi-modal expression pattern in male development. Furthermore, in the last molting of male (eclosion), genes in cluster 6 and 2 were abruptly upregulated, while genes in cluster 1 and 9 are downregulated dramatically. In addition, genes in cluster 3, 5, and 8 mostly expressed the highest levels in the 3rd instar nymph stage, those in cluster 1 and 9 exhibited their highest expression levels in

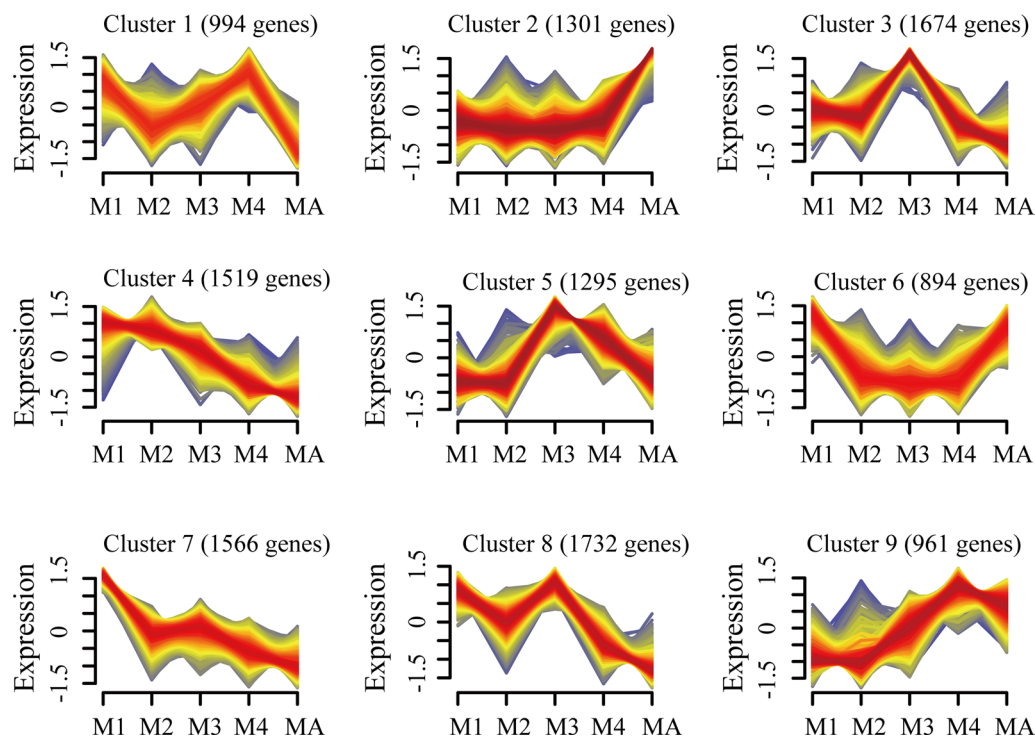


Fig. 5 Gene expression profiles across the development of male. Fuzzy c-means algorithm was implemented to cluster gene expression patterns in all developmental stages of male through Mfuzz software. The 11 936 genes expressed in male cotton aphid were divided into 9 distinct clusters of temporal patterns representing different expression kinetics

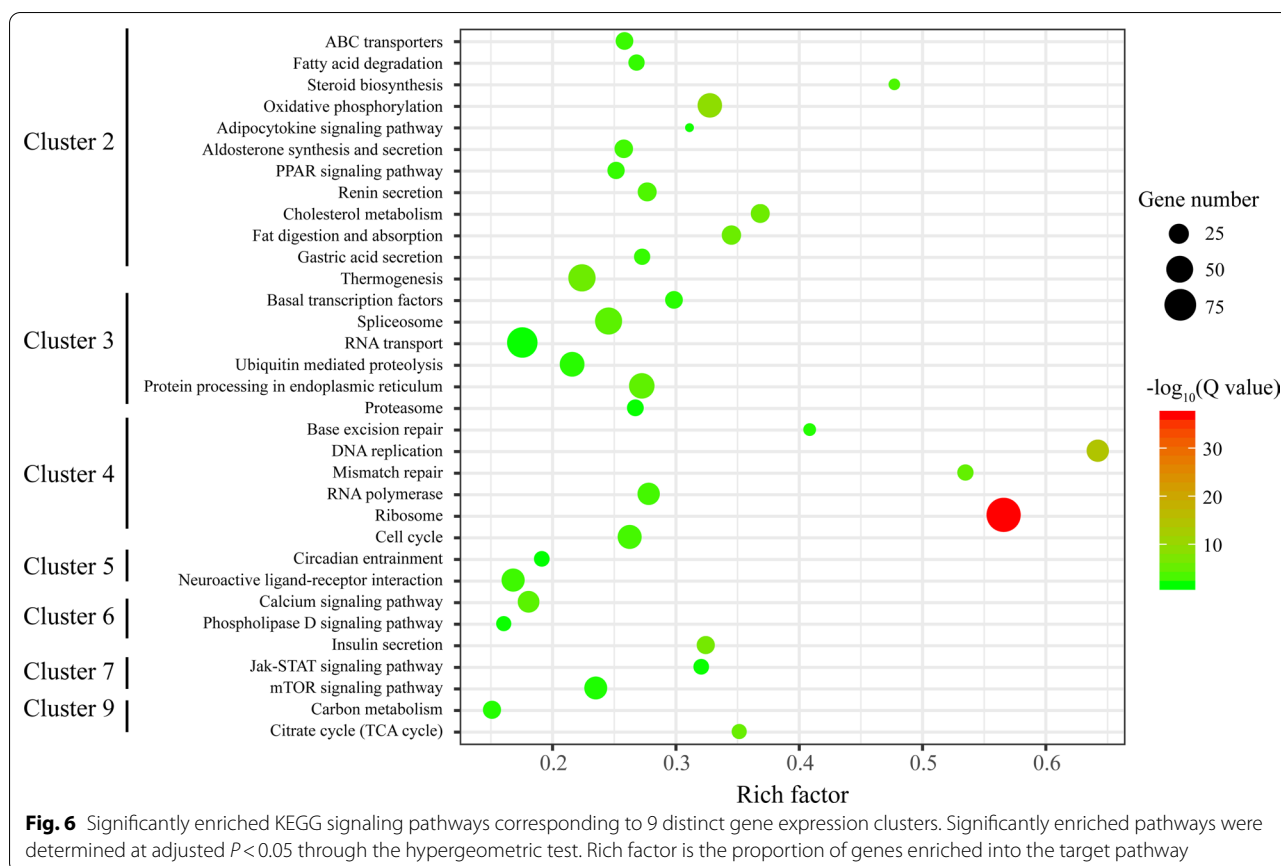
the 4th instar nymph stage, which were the two vital periods for wing wud formation and fully wing emergence in male, respectively.

KEGG signaling pathways enrichment was performed to reveal potential function of genes classified into the 9 clusters above (Fig. 6, Additional file 5: Table S5). Genes in cluster 2 were enriched in pathways of membranes transport (ABC transporters), lipid metabolism (fatty acid degradation, steroid biosynthesis), energy metabolism (oxidative phosphorylation), endocrine system (adipocytokine signaling pathway, aldosterone synthesis and secretion, PPAR signaling pathway, renin secretion), digestive system (cholesterol metabolism, fat digestion and absorption, gastric acid secretion), and environmental adaptation (thermogenesis). Cluster 3 and 4 genes were primarily associated with genetic information processing. Specifically, genes in cluster 3 involved in signaling pathways such as transcription (basal transcription factors, spliceosome), translation (RNA transport), “folding, sorting and degradation” (ubiquitin mediated proteolysis, protein processing in endoplasmic reticulum, proteasome), and genes in cluster 4 contributed to several vital signaling pathways such as replication and repair (base excision repair, DNA replication, mismatch repair), transcription (RNA polymerase), translation (ribosome),

cell growth and death (cell cycle). Genes in cluster 5 were related to pathways of the neuroactive ligand-receptor interaction and circadian entrainment. Cluster 6 and 7 genes were primarily taken part in signal transduction, in which calcium signaling pathway, phospholipase D signaling pathway, and insulin secretion were enriched in the former, while mTOR signaling pathway and Jak-STAT signaling pathway were enriched in the latter. At last, genes in cluster 9 participated in pathway of citrate cycle (TCA cycle) and carbon metabolism.

DEGs identification and function analysis across the male development

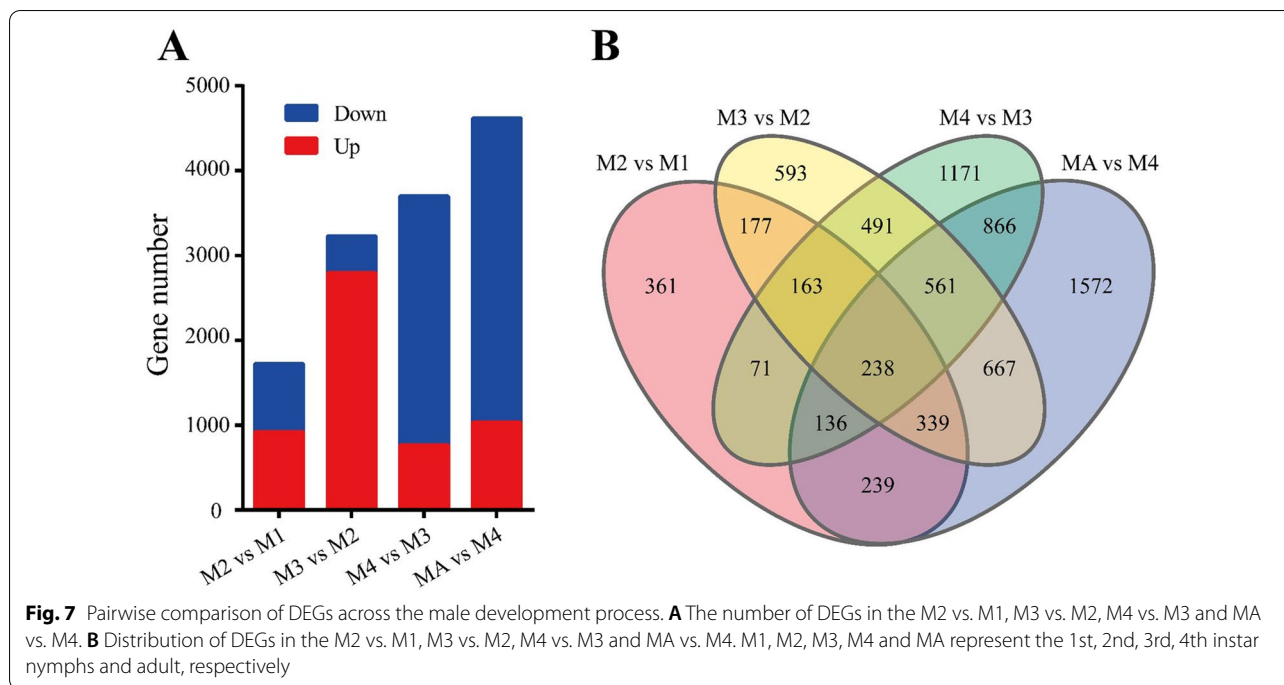
Compared with the 1st instar male, 921 genes were significantly up-regulated and 803 genes were significantly down-regulated in the 2nd instar male. When male nymph transformed from the 2nd instar to the 3rd instar, up to 3 229 significantly differentially genes were identified, in which 2 796 and 433 were up- and down-regulated, respectively. Moreover, with the drastic change of wing bud morphology, the expression levels of 765 and 2 932 genes were significantly higher and lower in the 4th instar male nymph than those in the 3rd instar male nymph, respectively. After the last molting, male adults became fully winged, in which 1 032 and 3 586 genes were



significantly up- down-regulated in comparison to the 4th instar nymph, respectively (Fig. 7A). Interestingly, the number of up-regulated genes in the development of males were increased and peaked at the pairwise between the 3rd instar and the 2nd instar (M3 vs M2), then decreased dramatically (M4 vs M3). Overlaps of DEGs among different pairwise comparison in five developmental stages of male were exhibited via Venn diagram (Fig. 7B). And 361, 593, 1 171, and 1 572 genes were exclusively significantly differentially expressed in comparison of the 2nd instar and the 1st instar (M2 vs. M1), the 3rd instar and the 2nd instar (M3 vs. M2), the 4th instar and the 3rd instar (M4 vs. M3), adult and the 4th instar (MA vs. M4), respectively.

The up- and down-regulated DEGs in the four pairwise comparison groups above were performed KEGG pathway enrichment separately (Fig. 8, Additional file 6: Table S6). In M2 vs. M1, mostly up-regulated DEGs were significantly enriched in organismal system (protein digestion and absorption, longevity regulating pathway, relaxin signaling pathway, ovarian steroidogenesis, dopaminergic synapse), cellular processes (Oocyte meiosis), while the down-regulated DEGs were involved in the immune system (Toll and Imd signaling pathway). For M3 vs. M2, the mainly up-regulated DEGs

were significantly enriched in environmental information processing (neuroactive ligand-receptor interaction, Ras signaling pathway), followed by organismal systems (dopaminergic synapse, circadian entrainment), while the down-regulated DEGs were significantly enriched in metabolism of phenylalanine and tyrosine, and steroid hormone biosynthesis. Compared with the 3rd instar nymph, the 4th instar male has up-regulated oxidative phosphorylation, thermogenesis, citrate cycle and carbon metabolism, whereas the regulated DEGs were primarily associated with genetic information processing of transcription, translation, replication and repair (i.e. DNA replication, mismatch repair, homologous recombination, RNA transport, etc.) (Additional file 6: Table S6). In comparison of the 4th instar nymph, the up-regulated DEGs adult males were mainly enriched in metabolism of lipid and carbohydrate (such as fatty acid metabolism, steroid hormone biosynthesis, pentose and glucuronate interconversions), digestive system (i.e. salivary secretion, fat digestion and absorption), endocrine system (i.e. signaling pathway of PPAR and GnRH), the down-regulated DEGs were significantly enriched in genetic information processing signaling pathway, such as Ribosome and RNA polymerase.

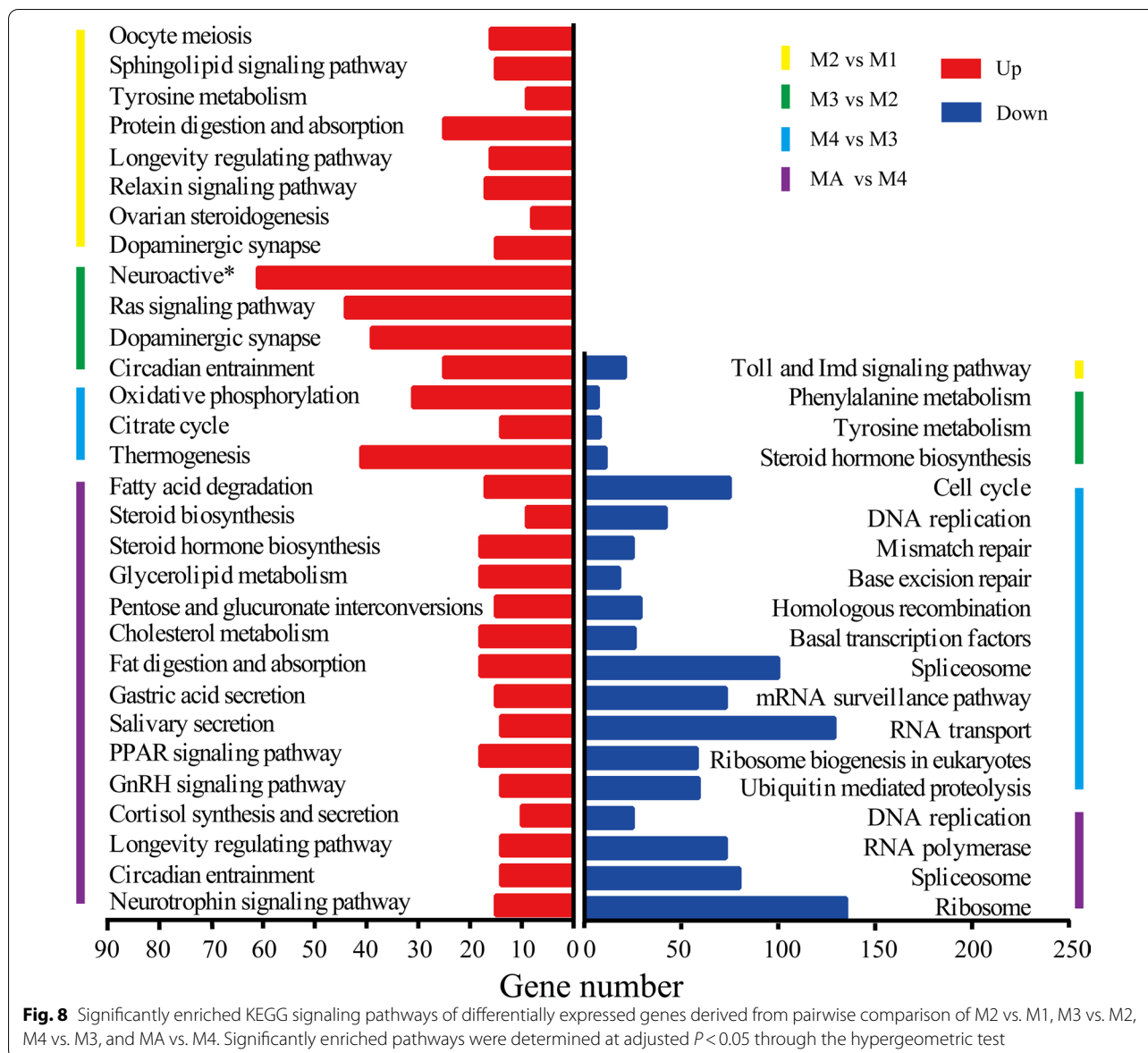


Weighted gene co-expression network analysis

To investigate the key modules of genes associated with wings formation in male, weighted gene co-expression network analysis was preformed, in which 7 645 co-expressed DEGs were divided into 17 modules (Fig. 9A and Additional file 7: Table S7). Genes with highly similar expression patterns are clustered together into the same module. Meanwhile, the pattern of gene expressions was often associated with phenotypic changes. The magenta module (70 genes) and salmon module (42 genes) were highly related to the 1st and 2nd instar nymphs. The blue module (165 genes), brown module (90 genes), pink module (71genes), black module (76 genes), purple module (59 genes), and red module (81 genes) was positively correlated with the 3rd instar nymph. The grey 60 module (29 genes), turquoise module (167 genes), green module (85 genes), and lightcyan module (30 genes), brown module (90 genes), pink module (71genes) were obviously associated with the 4th instar nymph. The grey 60 module (29 genes), turquoise module (167 genes), the midnightblue module (30 genes), yellow module (87 genes), tan module (46 genes), cyan module (32 genes), and greenyellow (52 genes) were primarily related to the 5th instar nymph (Fig. 9B).

To further identify the hub genes associated with phenotypic, a co-expression network was constructed and the connectivity patterns and hub genes of the relevant phenotypes were exhibited (Fig. 10). The Cytoscape

software visualization result showed that 31 genes were highly interactivity in the 1st and 2nd instar nymphs; 99 genes were highly interactivity in the 3rd instar nymph; 43 genes were highly interactivity in the 4th instar nymph. 53 hub genes were the most frequent interactions in the 5th instar nymph stage (Fig. 10). Top 10 hub genes as ranked by intra-module connectivity were showed in Table 2. In the 1st and 2nd instar nymphs, the most highly connected gene was *MCM4* (DNA replication licensing factor), followed by *MCM5* (DNA replication licensing factor), *CDC45* (cell division control protein 45), *POLD1* (DNA polymerase delta subunit 1). In the 3rd instar nymph, the *PLK1* (polo-like kinase 1) and *AURKA* were the most highly interactivity gene. In the 4th instar nymph, among the 10 top hub genes, *ADK* (adenosine kinase), *RSPH4A* (radial spoke head protein 4A), *HK* (hexokinase) and *KPNA2* (importin subunit alpha-2) were identified as the highly interactive gene. In the 5th instar nymph, *4CL* (4-coumarate-CoA ligase) was the most highly interactivity gene, followed by *YWHAB_Q_Z* (14-3-3 protein beta/theta/zeta), *PCK* (phosphoenolpyruvate carboxykinase (GTP)) and *SRPK3* (serine/threonine-protein kinase *SRPK3*). The gene expression patterns of 9 hub genes from the co-expression network analysis validated by qRT-PCR were significantly in accord with those obtained by RNA-seq mostly with the $R^2 > 0.6$ (Fig. 11).



Discussion

Morphology variation and wing bud differentiation of winged male

Males in Aphididae were usually neglected except for *A. pisum*, and only 731 species were recorded among more than 4 000 aphids (Blackman et al. 2007), of which 402, 317, 12 were exclusively winged (55%), wingless (43.36%), alternative wing (1.64%) (Fig. 1, Additional file 2: Table S2), which were defined as Class I, II, III here, respectively. Obviously, aphids of Class I such as *A. gossypii* were the representative species, which deserved to be explored further. In aphids, environmental conditions experienced during embryonic or nymphal stages determine the divergent adult phenotypes (Sutherland 1969).

To better understand wing differentiation of male cotton aphid, we systematically observed their wing development dynamics (Fig. 1). Their morphological changes across different stages were basically consistent with those observed in *A. pisum* and *Megoura viciae* (Ganassi et al. 2005a, b; Benedetti et al. 1991). In *A. gossypii* and *A. pisum*, obvious morphological changes of wing bud were found in the 3th instar nymph, and the wing buds located on thoracic sections of the 4th instar male can be observed clearly by naked eyes (Ishikawa et al. 2008). However, wing buds of *M. viciae* in the 4th instar nymph were similar to those in the 3rd instar, in which only the cells were more regularly arranged in two layers with again an evident slot between them. Specially, although

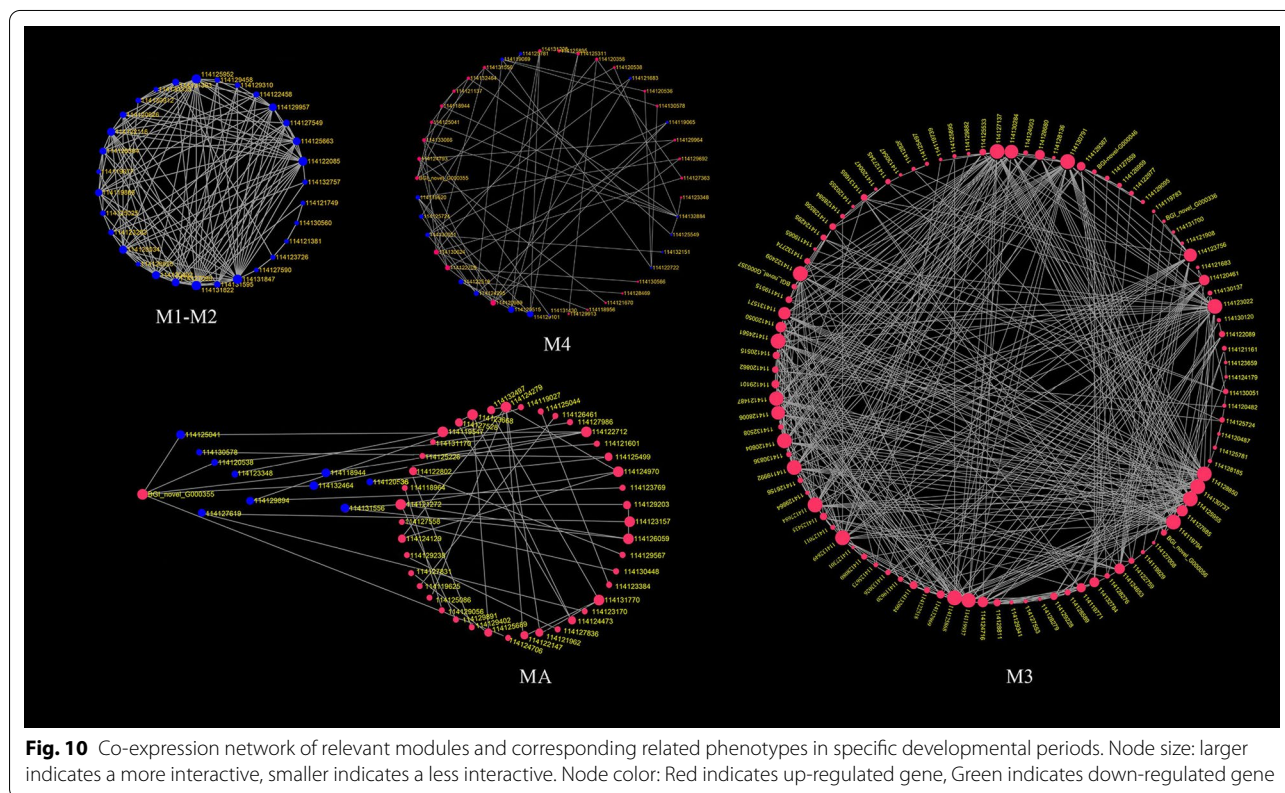
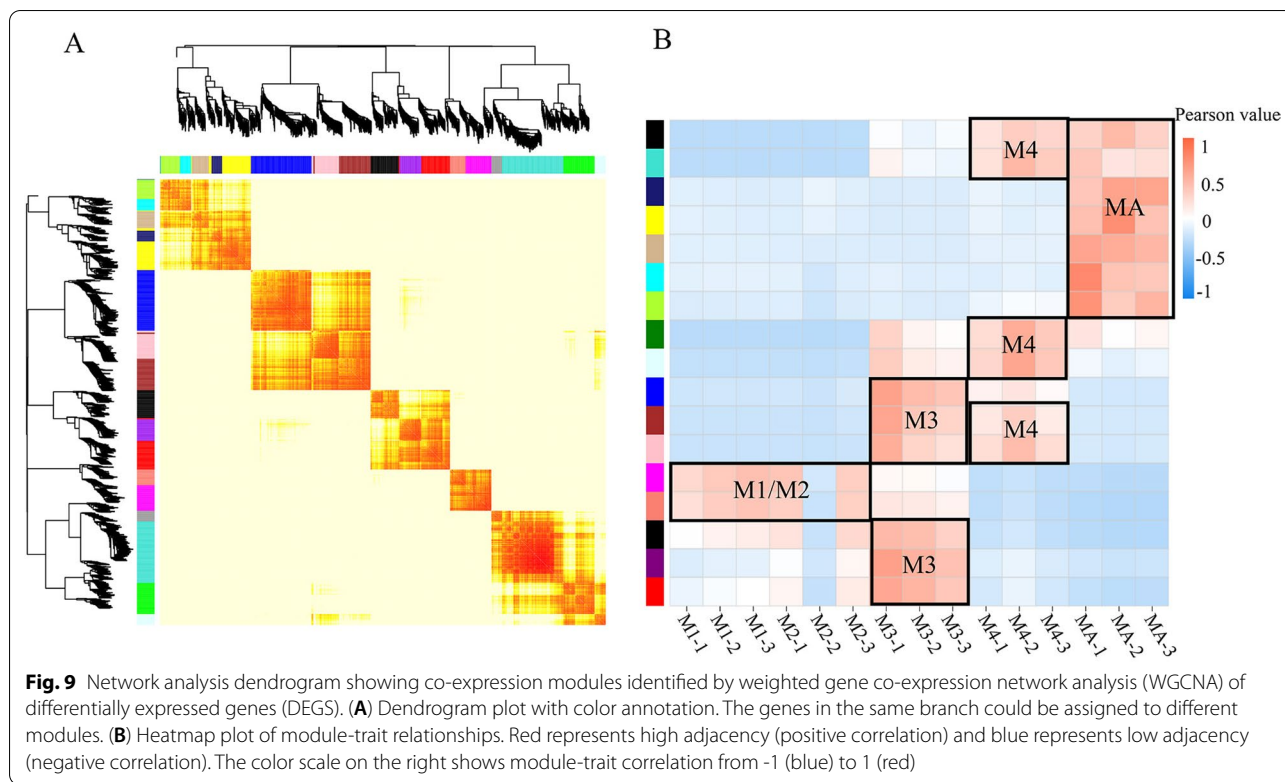


Table 2 The top 10 high interactive gene

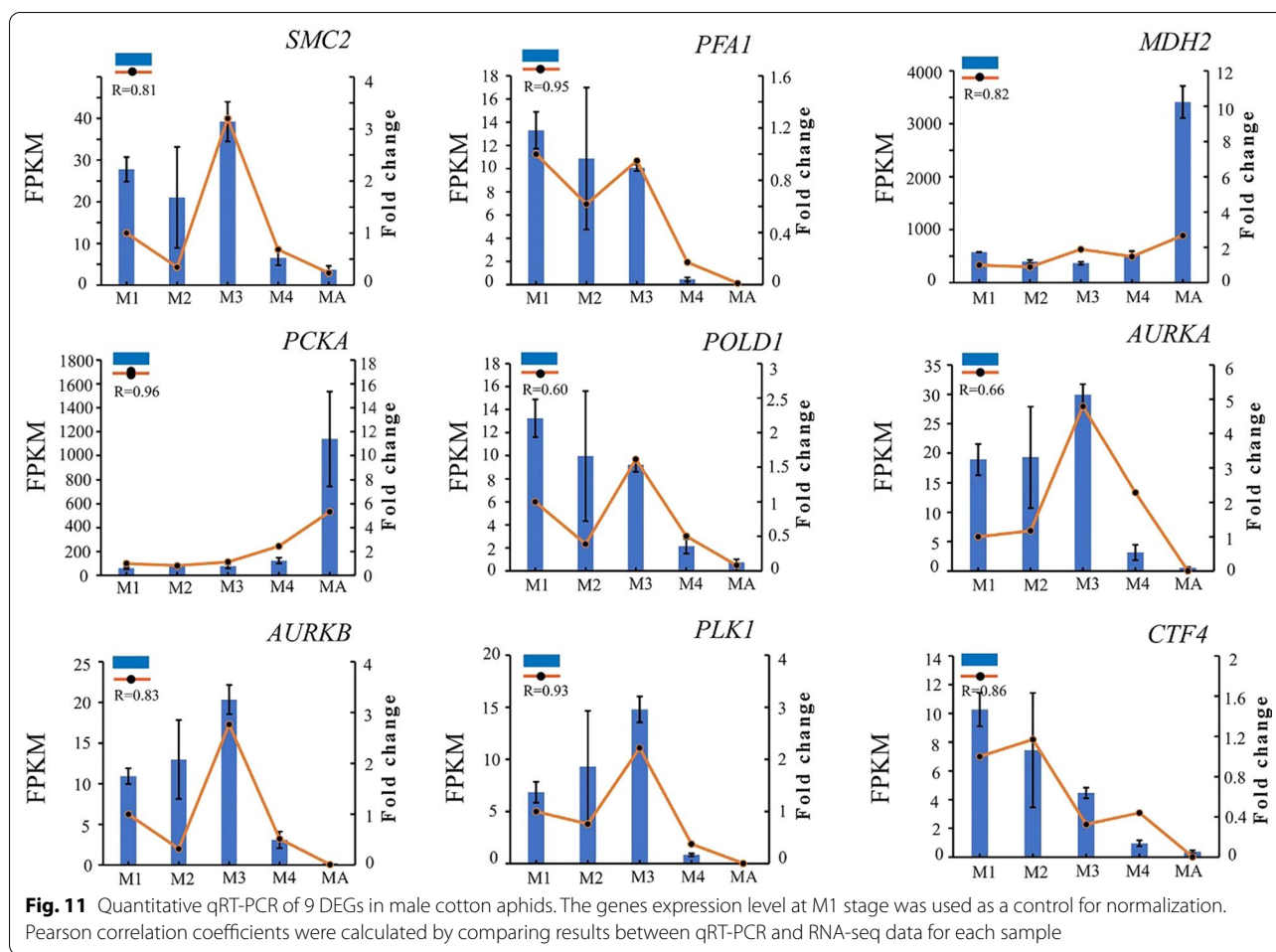
Sample	Gene ID	Gene name	Description
M1/2	114 131 847	MCM4	DNA replication licensing factor MCM4 [EC:3.6.4.12]
	114 131 822	MCM5	DNA replication licensing factor MCM5 [EC:3.6.4.12]
	114 125 952	CDC45	cell division control protein 45
	114 122 085	POLD1	DNA polymerase delta subunit 1 [EC:2.7.7.7]
	114 120 034	RFA1	replication factor A1
	114 122 116	MCM6	DNA replication licensing factor MCM6 [EC:3.6.4.12]
	114 120 492	RFA2	replication factor A2
	114 127 098	RRM1	ribonucleoside-diphosphate reductase subunit M1 [EC:1.17.4.1]
	114 125 663	CTF4	chromosome transmission fidelity protein 4
	114 119 866	ASPM	abnormal spindle-like microcephaly-associated protein
M3	114 127 137	PLK1	polo-like kinase 1 [EC:2.7.11.21]
	114 123 022	AURKA	Aurora kinase A [EC:2.7.11.1]
	114 130 791	KIF23	kinesin family member 23
	114 128 850	AURKB	Aurora kinase B [EC:2.7.11.1]
	114 125 955	BUB1	checkpoint serine/threonine-protein kinase [EC:2.7.11.1]
	114 119 794	KIF20	kinesin family member 20
	114,125,868	KIF18_19	kinesin family member 18/19
	114 119 992	SMC2	structural maintenance of chromosome 2
	114 132 849	TUBG	tubulin gamma
	114 120 604	ASPM	abnormal spindle-like microcephaly-associated protein
M4	114 132 884	ADK	adenosine kinase [EC:2.7.1.20]
	114 120 989	RSPH4A	radial spoke head protein 4A
	114,130,624	HK	hexokinase [EC:2.7.1.1]
	114 122 709	KPNA2	importin subunit alpha-2
	114 119 620	DNALI	dynein light intermediate chain, axonemal
	114 133 066	pfkA	6-phosphofructokinase 1 [EC:2.7.1.11]
	114 119 069	TOM70	mitochondrial import receptor subunit TOM70
	114 124 793	TEKT1	tektin-1
	114 124 295	DYX1C1	dyslexia susceptibility 1 candidate gene 1 protein
	114 129 101	DNAH	dynein heavy chain, axonemal
MA	114 124 279	4CL	4-coumarate-CoA ligase [EC:6.2.1.12]
	BGI_novel_G000355	YWHAB_Q_Z	14-3-3 protein beta/theta/zeta
	114 121 272	PCK	phosphoenolpyruvate carboxykinase (GTP) [EC:4.1.1.32]
	114 122 712	SRPK3	serine/threonine-protein kinase SRPK3 [EC:2.7.11.1]
	114 131 770	CHDH	choline dehydrogenase [EC:1.1.99.1]
	114 124 970	ACADM	acyl-CoA dehydrogenase [EC:1.3.8.7]
	114 123 668	MYO3	myosin III [EC:2.7.11.1]
	114 126 059	MDH2	malate dehydrogenase [EC:1.1.1.37]
	114 124 129	SDR16C5	all-trans-retinol dehydrogenase (NAD+) [EC:1.1.1.105]
	114 120 538	TSSK	testis-specific serine kinase [EC:2.7.11.1]

no significantly external morphological changes were observed in the 1st and 2nd instar nymphs of male cotton aphid, whereas a weeny wing bursa appeared on the prothorax of the 2nd instar male nymph, implying the development of wing primordia, which was consistent with previous reports that internal tissue structures already show differentiation from the 2nd instar onward (Ganassi *et al.* 2005a, b; Benedetti *et al.* 1991; Ishikawa

et al. 2008). These results suggest that the divergent adult phenotypes were probably determined in embryonic or neonatal stage.

Feeding behavior of winged male *A. gossypii*

The results of feeding behavior analysis showed that male cotton aphid produced 6 kinds of waveforms on cotton seedlings (Fig. 3). The puncture waveform of



male mouth needle outside the phloem (Pd, C, F waveform) contains the most probing numbers and longest duration time, which showed strong willingness to probe for feeding (Table 1). The puncture waveform of male needle in phloem (E1 and E2 waveform) contained the least number of puncture times and shortest duration time (Table 1), which indicated that although male has a strong desire to ingest, the feeding efficiency was lower. Consistent results have been reported in the comparison of the probing behaviors between alate and apterous of *M. persicae* on *Solanum tuberosum*, in which feeding activity of winged morph was lower (Boquel *et al.* 2011). Similar studies on aphid of *A. fabae* showed that the winged morph had higher feeding activity on the winter host (Powell *et al.* 2010). We hypothesized that lower feeding efficiency of male cotton aphid adults to the summer host (cotton) is probably due to enough energy that had been stored in nymphal stages or preference to winter host in adulthood. In fact, missions of wing male aphids are to migrate to winter host and mate with ovipara to

complete life cycle in turn. Exactly, the passive feeding waveform E2 has the least number of waves and the shortest duration, which also hints that winged male *A. gossypii* adults have low adaptability to summer host cottons.

Signaling pathway in critical period of wing differentiation of male *A. gossypii*

Transcriptomic dynamics across male cotton aphid development were obtained via RNA-seq. The largest number of up-regulated DEGs occurred during the development from the 2nd instar to 3rd instars (Fig. 7A), and time-course gene transcriptional pattern analysis results also showed that numerous genes in clusters 3, 5, and 8 had the highest expressed level in the 3rd instar stage (Fig. 5). Actually, dramatically morphological changes, especially the wing bud apophyses, can be observed from the 2nd instar to the 3rd instar (Fig. 2A). Hence, we speculated these highly expressed genes in the 3rd instar above probably determined the wing bud differentiation in male. Compared with the 2nd instar

nymph, the up-regulated DEGs in the 3rd instar nymph were enriched in neuroactive ligand-receptor interaction and Ras signaling pathway, dopaminergic synapse, and circadian entrainment (Fig. 8, Additional file 6: Table S6). Furthermore, highest expressed genes in the 3rd instar (cluster 3, 5, 8) were mostly involved in genetic information processing, followed by organismal systems and environmental information processing (Fig. 5, Additional file 5: Table S5). Obviously, those signaling pathway accelerate wing bud differentiation and development collaboratively and should get receive more attention in future.

From the 3rd, 4th instar to adult, the number of down-regulated DEGs were larger than up-regulated DEGs (Fig. 7A). Interestingly, the up-DEGs were mostly related to organismal systems, lipid metabolism, carbohydrate metabolism, energy metabolism (Additional file 6: Table S6). In addition, the down-regulated DEGs were mostly associated with genetic information processing including translation, replication and repair (Additional file 6: Table S6). These results indicated that the ability of cell and some tissue differentiation decreases with the maturation of aphid internal organs, and the entirely metabolism strengthen meanwhile. Specially, in MA vs. M4, the large number of up-regulated DEGs were mainly enriched in the fatty acid metabolism, fat digestion and absorption, PPAR signaling pathway, steroid hormone biosynthesis, glycerolipid metabolism and so on (Fig. 8). These signaling pathways were also reported significantly up-regulated in alate brown citrus aphid *Toxoptera citricida* and in long winged *Sogatella furcifera* (Shang et al. 2016; Liang et al. 2018). Moreover, silencing of lipid synthesis and degradation genes in *T. citricida* leading to underdeveloped wings revealed that both lipid metabolism and energy supply are essential for aphid wing bud differentiation (Shang et al. 2016; Liang et al. 2018).

Candidate hub genes of wing differentiation in males

WGCNA were used to identify the specifically expressed hub genes potentially involved in wing differentiation of male in *A. gossypii* among 7 645 DEGs, and the top 10 ones are shown as the order of interactivity in Table 2. Among the top 10 nodes in the younger larval stages (the 1st and 2nd instar nymphs), the *CDC45*, *POLD1*, *RFA1*, *RFA2*, *RRM1*, *CTF4*, *ASPM*, and the mini-chromosome maintenance (MCM) gene family members (*Mcm4*, *Mcm5*, *Mcm6*) were identified as candidate hub genes. *CDC45* is an essential gene for the initiation of DNA replication and elongation (Luis and Ponting 2011). *Cdc45* can bind to *Mcm2-7* and GINS proteins to form a complex that is competent to unwind double stranded DNA and regulate DNA replication (Petojevic et al. 2015). The phenotype of lacking functional *CDC45* gene was

reported in the mice, and the loss of *CDC45* gene function impaired proliferation of the inner cell mass (Yoshida et al. 2001). The *MCM* gene family play an important role in eukaryotes DNA replication, and silencing of *Mcm4* results in inhibition of *de novo* DNA synthesis and polyploidization, and arrested oocyte maturation and ovarian growth in the migratory locust (Guo et al. 2014). The *POLD1* gene (also known as *CDC2*) encodes the catalytic subunit of eukaryotic DNA polymerase- δ , and previous studies have shown that the *POLD1* mutation was significantly impeded the growth and proliferative ability of the cells (Liu et al. 2020; Song et al. 2009). In addition, The *RFA1*, *RFA2*, *RRM1*, *CTF4*, and *ASPM*, are involved in eukaryotes DNA replication and cell proliferation (Longhese et al. 1994; Lei et al. 2012; Villa et al. 2016; Pan et al. 2008). In summary, all 10 candidate hub genes in younger larval stages (the 1st to 2nd instar stage) are involved in DNA replication and cell proliferation. Combined with the morphological study above, these candidate hub genes probably respond to the environment-induced wing plasticity in the embryonic stage, the 1st and 2nd instar nymphal stage. However, it remains to be determined how they respond to the environment-induced and regulate the early development of wing buds during the preliminary stage.

In the 3rd instar nymph, the wing buds begin to develop further and the obvious morphological changes of wing bud were observed. The genes related to cell division, sister chromatid cohesion, mitotic entry such as *PLK1*, *BUB1*, *SMC2*, *TUBG*, *ASPM*, the kinesin family members (KIF23, KIF20, KIF18-19) and the novel subfamily of serine/threonine (Aurora kinase A and Aurora kinase B) were identified as candidate hub genes potentially involved into wing development in the prophase (Table 2). However, these core genes involved in cell division and sister chromatid separation have been poorly studied in insects. Hence, how they regulate the wing differentiation need to be further explored. Studies in mammalian cells have shown that the loss of *PLK1* function leads to a short delay entry into mitosis and subsequently often die by apoptosis (Sumara et al. 2004). In the *Plk1*-depleted cells, Aurora B inhibitor can silence the spindle checkpoint by stabilizing microtubule kinetochore interaction, and the cell exiting mitosis without chromosome segregation and cytokinesis (Sumara et al. 2004). *Bub1* as a multi-task protein kinase plays an important role in mammalian chromosomal instability (Kawashima et al. 2010). The *SMC2*, *TUBG*, *ASPM*, the kinesin family members (KIF23, KIF20, KIF18-19) and the novel subfamily of serine/threonine (Aurora kinase A and Aurora kinase B) has been reported to be mainly associated with chromosome segregation, condensation and cell cycle in

mammals (Pan et al. 2008; Strunnikov et al. 1995; Joshi et al. 1992; Zhu et al. 2020; Martin et al. 2013; Goldenson et al. 2014). To sum up, we hypothesized that these genes probably regulate the further development of wing buds by regulating cell division, sister chromatid cohesion and mitotic entry.

In the 4th instar nymph, the wing buds located on thoracic sections of male can be observed clearly by naked eyes. *RSPH4A*, *KPNA2*, *DNALI*, *TOM70*, *TEKT1*, *DYX1C1*, *DNAH*, and three kinase genes (*ADK*, *HK*, *pfkA*) showed high network interaction (Table 2). The *RSPH4A*, *DNALI*, and *DNAH* were reported to be closely related to the movement of cilia and sperm axoneme, and the loss of genes function led to male and female subfertility (Castleman et al. 2009; Rashid et al. 2006; Whitfield et al. 2019). Similarly, loss of *TEKT1* gene function in *Bactrocera dorsalis* was also reported to lead to male infertility (Sohail et al. 2019). Interestingly, the *DNALI* and *TEKT1* were highly expressed in male testis (Rashid et al. 2006; Sohail et al. 2019). Combining the functions of these genes and the high interactivity of these genes in the 4th instar nymphal stage suggests that the male cotton aphid not only undergo the further development of wings, but also undergo the development of the male reproductive system. In addition, these genes related to the glucose homeostasis and energy metabolism (*HK* and *pfkA*) also play a vital role in providing energy for flight muscle (Storey 1980; Siedler et al. 2012; Dixon et al. 1993). Transcriptome studies of *Sogatella furcifera* have shown consistent results that genes associated with energy metabolism and flight muscle is crucial in plasticity development of wing (Gao et al. 2019). Another study in brown planthopper and *S. furcifera* have shown that insulin signaling genes also play an important role in the differentiation of wing type (Gao et al. 2019; Xu et al. 2015). In recent years, juvenile hormone and ecdysone signaling have also been shown to be involved in the development of wing plasticity (Zhang et al. 2019; Vellichirammal et al. 2017).

After last molting, adult male emerged with full wings. The genes associated with energy metabolism such as *YWHAB_Q_Z*, *PCK*, *ACADM*, and *MDH2* showed high network interaction (Table 2). On the whole, the energy utilization of insects in flight can be divided into three types: sugar utilization type, fat utilization type and both of them. Locusts use carbohydrates and fat as the energy supply for initial flight and continuous flight, respectively (Rowan et al. 1979). However, when the flight energy is transformed from carbohydrate to fat, the carbohydrate is not simply exhausted, and a certain carbohydrate reserve can provide energy for the sudden flight behavior of insects (Michel et al. 1986; Liu et al. 2007; Mayer et al. 1969). In the study, genes associated with

gluconeogenesis (*YWHAB_Q_Z*) (Ji et al. 2021) and fatty acid metabolism (*PCK*, *ACADM*, and *MDH2*) (Schmidt et al. 1981; Zhang et al. 2015) showed high network interaction implied that these genes played an important role in flight energy supply in winged male adult of cotton aphid. In particular, genes related to fatty acid biosynthesis and metabolism, namely *ACADM* and *MDH2*, are crucial in long periods of flight for finding primary hosts. *TSSK1* and *CHDH* are two genes associated with male reproduction (Sohail et al. 2019; Johnson et al. 2010). The high interactivity of these reproductive-related genes also corresponded to the previous reports that the morphological plasticity of insect was accompanied by reproductive plasticity in response to environmental changes (Tufail et al. 2010).

Conclusion

The study explored morphological and transcriptional dynamics of male cotton aphids in the development, and revealed the phenomenon of low feeding efficiency of winged male cotton aphids on summer hosts. Dynamic transcriptome analysis of male aphid at 5 different developmental periods showed that the 3rd instar nymphs were the critical stage of wing bud differentiation in males. Pathway enrichment analysis of DEGs and weighted gene co-expression network analysis revealed key signaling pathway and candidate hub genes that may be involved in wing differentiation in males of cotton aphid.

Supplementary Information

The online version contains supplementary material available at <https://doi.org/10.1186/s42397-022-00130-x>.

Additional file 1: Table S1 The designed primers for qRT-PCR.

Additional file 2: Table S2 The taxonomic statistics of male aphid.

Additional file 3: Table S3 The statistics of developmental period and morphological data of male aphid.

Additional file 4: Table S4 Summary statistics of RNA-seq results in developing *A. gossypii*.

Additional file 5: Table S5 Gene clusters and enriched pathways.

Additional file 6: Table S6 Enriched KEGG pathways in comparison between different developmental stages.

Additional file 7: Table S7 Gene information statistics of different modules of WGCNA cluster.

Acknowledgements

We thank the editors and reviewers for all their constructive comments on our work. This research was funded by National Natural Science Foundation of China (No. 32102214) and Special Fund for Basic Public Welfare Research of Institute of Cotton Research of CAAS (No. 1610162020020604). Studies were carried out in laboratories at the Institute of Cotton Research of CAAS, Anyang, China.

Author contributions

Ji JC, Ma XY, Cui JJ, and Luo JY conceived and designed the research; Huangfu NB and Ji JC collected the samples. Ji JC, Shi QY, and Chen LL conducted

experiments. Ji JC and Huangfu NB analyzed the data. Huangfu NB and Ji JC wrote the paper. All authors have read and approved the manuscript.

Declarations

Ethics approval and consent to participate

We declare that our study was conducted in strict compliance with ethical standards. Collection of *A. gossypii* in this study did not require permits because it is a common cotton pest in China.

Competing interests

All authors declare that they have no conflict of interest.

Author details

¹Zhengzhou Research Base, State Key Laboratory of Cotton Biology, Zhengzhou University, Zhengzhou 450001, China. ²State Key Laboratory of Cotton Biology, Institute of Cotton Research, Chinese Academy of Agricultural Sciences, Anyang, Henan 455000, China. ³College of Agronomy, Xinjiang Agricultural University, Urumqi 830052, China.

Received: 18 April 2022 Accepted: 26 July 2022

Published online: 15 September 2022

References

- Altschul SF, Gish W, Miller W, et al. Basic local alignment search tool. *J Mol Biol.* 1990;215:403–10. <https://doi.org/10.1016/S0022-2836>.
- Ardie J. Life Cycles and Polyphenism. In: van Emden HF, Harrington R, editors. *Aphids as crop pests*. 2nd ed. Oxfordshire: CABI; 2017. p. 81–97.
- Benedetti I, Cova S, Mola L, et al. Chronology of wing development in *Megoura viciae* Buckt and *Acyrtosiphon pisum* Harris (Homoptera: Aphididae). In: *Atti del XVI Congresso Nazionale di Entomologia, Bari-Martina Franca*. 1991; 239–243.
- Blackman RL, Eastop VF. *Aphids on the World's trees*. *Crop Prot.* 2006;15(4):400–400. [https://doi.org/10.1016/0261-2194\(96\)89825-5](https://doi.org/10.1016/0261-2194(96)89825-5).
- Boquel S, Giordanengo P, Ameline A. Probing behavior of apterous and alate morphs of two potato-colonizing aphids. *J Insect Sci.* 2011;11(1):164. <https://doi.org/10.1673/031.011.16401>.
- Braendle C, Caillaud MC, Stern DL. Genetic mapping of aphicarus—a sex-linked locus controlling a wing polymorphism in the pea aphid (*Acyrtosiphon pisum*). *Heredity.* 2005;94(4):435–42. <https://doi.org/10.1038/sj.hdy.6800633>.
- Braendle C, Davis GK, Brisson JA, et al. Wing dimorphism in aphids. *Heredity.* 2006;97(3):192. <https://doi.org/10.1038/sj.hdy.6800863>.
- Castleman VH, Romio L, Chodhari R, et al. Mutations in radial spoke head protein genes *RSPH9* and *RSPH4A* cause primary ciliary dyskinesia with central-microtubular-pair abnormalities. *Am J Human Genetics.* 2009;84(2):197–209. <https://doi.org/10.1016/j.ajhg.2009.01.011>.
- Chen YZ, Vanlerberghe-Masutti F, Wilson LJ, et al. Evidence of superclones in Australian cotton aphid *Aphis gossypii* glover (*Aphididae: Hemiptera*). *Pest Manag Sci.* 2013;69(8):938–48. <https://doi.org/10.1126/science.1187881>.
- Dewey CN, Li B. RSEM: accurate transcript quantification from RNA-Seq data with or without a reference genome. *BMC Bioinformatics.* 2011;12(1):323–323. <https://doi.org/10.1186/1471-2105-12-323>.
- Ding BY, Shang F, Zhang Q, et al. Silencing of two insulin receptor genes disrupts nymph-adult transition of alate brown citrus aphid. *Int J Mol Sci.* 2017;18(2):357. <https://doi.org/10.3390/ijms18020357>.
- Dixon AFG, Horth S, Kindlmann P. Migration in insects: cost and strategies. *J Anim Ecol.* 1993;62(1):182–90.
- Elisa G, Aranzazu M, Sara H, et al. Electrical penetration graph technique as a tool to monitor the early stages of aphid resistance to insecticides. *Pest Manage Sci.* 2016;72(4):707–18. <https://doi.org/10.1002/ps.4041>.
- Ganassi S, Signa G, Mola L. Development of the wing buds in *Megoura viciae*: a morphological study. *Bull Insectol Bull Insectol.* 2005b;58(2):101–5.
- Ganassi S, Signa G, Mola L. Development of the wing buds in *Megoura viciae*: a morphological study. *Bull Insectol.* 2005b;58(2):101–5.
- Gao XL, Fu YT, Ajayi OE, et al. Identification of genes underlying phenotypic plasticity of wing size via insulin signaling pathway by network-based analysis in *Sogatella furcifera*. *BMC Genomics.* 2019;20(1):1–20. <https://doi.org/10.1186/s12864-019-5793-z>.
- Gao XK, Zhang S, Luo JY, et al. Identification and validation of reference genes for gene expression analysis in *Aphidius gifuensis* (Hymenoptera: Aphididae). *PLoS ONE.* 2017;12(11):e0188477. <https://doi.org/10.1371/journal.pone.0188477>.
- Goldenson B, Crispino JD. The aurora kinases in cell cycle and leukemia. *Oncogene.* 2014;34(5):1–9. <https://doi.org/10.1038/onc.2014.14>.
- Guo W, Wu ZX, Song JS, et al. Juvenile hormone-receptor complex acts on Mcm4 and Mcm7 to promote polyploidy and vitellogenesis in the migratory locust. *PLoS Genet.* 2014;10(10):e1004702. <https://doi.org/10.1371/journal.pgen.1004702>.
- Horvath S, Dong J, Miyano S. Geometric interpretation of gene co-expression network analysis. *PLoS Comput Biol.* 2008;4(8):e1000117. <https://doi.org/10.1371/journal.pcbi.1000117>.
- Ishikawa A, Hongo S, Miura T. Morphological and histological examination of polyphenic wing formation in the pea aphid *Acyrtosiphon pisum* (Hemiptera, Hexapoda). *Zoomorphology.* 2008;127(2):121–33. <https://doi.org/10.1007/s00435-008-0057-5>.
- Ji JC, Huangfu NB, Luo JY, et al. Insights into wing dimorphism in worldwide agricultural pest and host-alternating aphid *Aphis gossypii*. *J Cotton Res.* 2021;4(1):1–12. <https://doi.org/10.1186/s42397-021-00083-7>.
- Ji LL, Wang QQ, Liu MG, et al. The 14–3–3 protein YWHAB inhibits glucagon-induced hepatic gluconeogenesis through interacting with the glucagon receptor and FOXO1. *FEBS Lett.* 2021;595:1275–88. <https://doi.org/10.1002/1873-3468.14063>.
- Johnson B, Birks PR. Studies on wing polymorphism in aphids I. The developmental process involved in the production of the different forms. *Entomol Exp Appl.* 1960;3:327–39. <https://doi.org/10.1111/j.1570-7458.1960.tb00461.x>.
- Johnson AR, Craciunescu CN, Guo Z, et al. Deletion of murine choline dehydrogenase results in diminished sperm motility. *FASEB J.* 2010;24:2752–61. <https://doi.org/10.1096/fj.09-153718>.
- Joshi HC, Palacios MJ, Mcnamara L, et al. γ -tubulin is a centrosomal protein required for cell cycle-dependent microtubule nucleation. *Nature.* 1992;356(6364):80–3. <https://doi.org/10.1038/356080a0>.
- Kawashima SA, Yamagishi YY, Honda T, et al. Phosphorylation of H2A by Bub1 prevents chromosomal instability through localizing shugoshin. *Science.* 2010;327(8):172–7. <https://doi.org/10.1126/science.1180189>.
- Kim D, Langmead B, Salzberg SL. HISAT: a fast spliced aligner with low memory requirements. *Nat Methods.* 2015;12(4):357–60. <https://doi.org/10.1038/nmeth.3317>.
- Kwon SH, Kim DS. Effects of temperature and photoperiod on the production of sexual morphs of *Aphis gossypii* (Hemiptera: Aphididae) in Jeju. *Korea J Asia-Pacific Entomol.* 2017;20:53–6. <https://doi.org/10.1016/j.aspen.2016.11.006>.
- Langfelder P, Horvath S. WGCNA: an R package for weighted correlation network analysis. *BMC Bioinformatics.* 2008;9(1):559. <https://doi.org/10.1186/1471-2105-9-559>.
- Langmead B, Salzberg SL. Fast gapped-read alignment with Bowtie 2. *Nat Methods.* 2012;9(4):357–9. <https://doi.org/10.1038/nmeth.1923>.
- Lee Y, Lee W, Lee S, et al. A cryptic species of *Aphis gossypii* (Hemiptera: Aphididae) complex revealed by genetic divergence and different host plant association. *Bull Entomol Res.* 2015;105(1):40–51. <https://doi.org/10.1017/S0007485314000704>.
- Lei W, Feng XH, Deng WB, et al. Progesterone and DNA damage encourage uterine cell proliferation and decidualization through up-regulating ribonucleotide reductase 2 expression during early pregnancy in mice. *J Biol Chem.* 2012;19:15174–92. <https://doi.org/10.1074/jbc.M111.308023>.
- Liang AW, Zhang H, Lin J, et al. De novo assembly and analysis of the white-backed planthopper (*Sogatella furcifera*) transcriptome. *J Insect Sci.* 2018;18:1–7. <https://doi.org/10.1093/jisesa/iey074>.
- Liu J, Liu Y, Fu JX, et al. Preliminary study on the function of the *POLD1* (CDC2) EXON2 c56G>A mutation. *Molecul Genetic Genomic Med.* 2020;8(8):1280. <https://doi.org/10.1002/mgg3.1280>.
- Liu H. Flight ability and some related physiological mechanism in social type and scattered type *Locusta migratoria* manilensis. Beijing: Chinese Academy of Agricultural Sciences. 2007.
- Livak KJ, Schmittgen TD. Analysis of relative gene expression data using real time quantitative PCR and the $2^{-\Delta\Delta CT}$ method. *Methods.* 2001;25(4):402–8.

- Lokesh K, Matthias F. Mfuzz: a software package for soft clustering of microarray data. *Bioinform Open Access Forum*. 2007;2:5–7. <https://doi.org/10.6026/97320630002005>.
- Longhese MP, Plevani P, Lucchini G. Replication factor A is required in vivo for DNA replication, repair, and recombination. *Mol Cell Biol*. 1994;14(12):7884–90. <https://doi.org/10.1155/S0962935194000657>.
- Love MI, Huber W, Anders S. Moderated estimation of fold change and dispersion for RNA-seq data with DESeq2. *Genome Biol*. 2014;15(12):550. <https://doi.org/10.1186/s13059-014-0550-8>.
- Lu YH, Wu KM, Jiang YY, et al. Mirid bug outbreaks in multiple crops correlated with wide-scale adoption of Bt cotton in China. *Science*. 2010;328:1151–4.
- Luis SP, Ponting CP. Cdc45: the missing RecJ ortholog in eukaryotes? *Bioinformatics*. 2011;27:1885–8. <https://doi.org/10.1093/bioinformatics/btr332>.
- Martin F, Inga G, Sindy S, et al. p53 and cell cycle dependent transcription of kinesin family member 23 (KIF23) is controlled via a CHR promoter element bound by DREAM and MMB complexes. *PLoS ONE*. 2013;8(5):e63187. <https://doi.org/10.1371/journal.pone.0063187>.
- Mayer RJ, Candy DJ. Changes in energy reserves during flight of the desert locust. *Schistocerca Gregaria Comparative Biochem Physiol*. 1969;31(3):409–18. <https://doi.org/10.1016/0010-406X>.
- Michel R, Beinhauer I, Andreas K, et al. The regulation of glycolysis in flying locusts (*Locusta migratoria*). *Biochim Soc Trans*. 1986;14(6):1078–9. <https://doi.org/10.1042/bst0141078>.
- Ogawa K, Miura T. Two developmental switch points for the wing polymorphisms in the pea aphid *Acyrtosiphon pisum*. *EvoDevo*. 2013;4:30. <https://doi.org/10.1186/2041-9139-4-30>.
- Pan HW, Lin SY, Chou HY, et al. ASPM (abnormal spindle-like, microcephaly-associated) gene encoding a centrosome protein is involved in cell proliferation, tumor cell invasion and overexpressed in HCC. *J Hepatol*. 2008;537. [https://doi.org/10.1016/S0168-8278\(08\)60086-0](https://doi.org/10.1016/S0168-8278(08)60086-0).
- Pertea R, Pertea GM, Antonescu CM, et al. StringTie enables improved reconstruction of a transcriptome from RNA-seq reads. *Nat Biotechnol*. 2015;33(3):290–5. <https://doi.org/10.1038/nbt.3122>.
- Petojevic T, Pesavento JJ, Costa A, et al. Cdc45 (cell division cycle protein 45) guards the gate of the Eukaryote Replisome helicase stabilizing leading strand engagement. *Proc Natl Acad Sci USA*. 2015;112:249–58. <https://doi.org/10.1073/pnas.1422003112>.
- Powell G, Hardie J. A potent, morph-specific parturition stimulant in the overwintering host plant of the black bean aphid. *Aphis Fabae Physiol Entomol*. 2010;26(3):194–201. <https://doi.org/10.1046/j.0307-6962.2001.00234.x>.
- Prado E, Tjallingii WF. Aphid activities during sieve element punctures. *Entomol Exp Appl*. 1994;72:157–65.
- Quan Q, Hu X, Pan B, et al. Draft genome of the cotton aphid *Aphis gossypii*. *Insect Biochem Mol Biol*. 2019;105:25–32. <https://doi.org/10.1016/j.ibmb.2018.12.007>.
- Rashid S, Breckle R, Hupe M, et al. The murine Dnal1 gene encodes a flagellar protein that interacts with the cytoplasmic dynein heavy chain 1. *Mol Reprod Dev*. 2006;73(6):784–94. <https://doi.org/10.1002/mrd.20475>.
- Reiner A, Yekutieli D, Benjamini Y. Identifying differentially expressed genes using false discovery rate controlling procedures. *Bioinformatics*. 2003;19(3):368–75. <https://doi.org/10.1093/bioinformatics/btf877>.
- Rowan AN, Newsholme EA. Changes in the contents of adenine nucleotides and intermediates of glycolysis and the citric acid cycle in flight muscle of the locust upon flight and their relationship to the control of the cycle. *Biochem J*. 1979;178(1):209–16. <https://doi.org/10.0000/PMID435278>.
- Sarria E, Cid M, Garzo E, et al. Excel workbook for automatic parameter calculation of EPG data. *Comput Electron Agric*. 2009;72(2):157–65. <https://doi.org/10.1111/j.1570-7458.1994.tb01813.x>.
- Schmidt J, Reinsch J, McFarland JT. Mechanistic studies on fatty acyl-CoA dehydrogenase. *J Biol Chem*. 1981;256(22):11667. <https://doi.org/10.1016/0165-022X>.
- Shang F, Ding BY, Xiong Y, et al. Differential expression of genes in the alate and apterous morphs of the brown citrus aphid. *Toxoptera Citricida Sci Report*. 2016;6:32099. <https://doi.org/10.1038/srep32099>.
- Shull AF. Time of determination and time of differentiation of aphid wings. *Am Nat*. 1938;72(739):170–9. <https://doi.org/10.1086/280774>.
- Siedler S, Bringermeier S, Bott M. Reductive whole-cell biotransformation with *Corynebacterium glutamicum*: improvement of NADPH generation from glucose by a cyclized pentose phosphate pathway using *pfkA* and *gapA* deletion mutants. *Appl Microbiol Biotechnol*. 2013;97(1):143–52. <https://doi.org/10.1007/s00253-012-4314-7>.
- Sohail S, Tariq K, Zheng WW, et al. RNAi-mediated knockdown of Tssk1 and Tektin1 genes impair male fertility in *Bactrocera dorsalis*. *Insects*. 2019;10(6):1–13. <https://doi.org/10.3390/insects10060164>.
- Song NM, Zhu XY, Shi L, et al. Identification and functional analysis of CDE/CHR elements in pold1 gene promoter. *Sci China Press*. 2009;39(5):449–59. <https://doi.org/10.1007/s11427-009-0077-5>.
- Storey KB. Regulatory properties of hexokinase from flight muscle of *Schistocerca americana gregaria* Role of the enzyme in control of glycolysis during the rest-to-flight transition. *Insect Biochem*. 1980;10(6):637–45. [https://doi.org/10.1016/0020-1790\(80\)90053-0](https://doi.org/10.1016/0020-1790(80)90053-0).
- Strunnikov AV, Hogan E, Koshland D. SMC2, a *Saccharomyces cerevisiae* gene essential for chromosome segregation and condensation, defines a subgroup within the SMC family. *Genes Dev*. 1995;9(5):587–99. <https://doi.org/10.1101/gad.9.5.587>.
- Sumara I, Giménez-Abián JF, Gerlich D, et al. Roles of polo-like kinase 1 in the assembly of functional mitotic spindles. *Current Biology Cb*. 2004;14(19):1712–22. <https://doi.org/10.1016/j.cub.2004.09.049>.
- Sun YC, Guo HJ, Yuan L, et al. Plant stomatal closure improves aphid feeding under elevated CO₂. *Glob Change Biol*. 2015;21(7):2739–48. <https://doi.org/10.1111/gcb.12858>.
- Sutherland ORW. The role of crowding in the production of wing forms by two strains of the pea aphid. *Acyrtosiphon Pisum J Insect Physiol*. 1969;15(8):1385–410. [https://doi.org/10.1016/0022-1910\(69\)90199-1](https://doi.org/10.1016/0022-1910(69)90199-1).
- Tjallingii WF. Electrical recording of stylet penetration activities aphids, their biology, natural enemies and control. In: Minks AK, Harrewijn P, editors. *Aphids, their biology, natural enemies and control*. Amsterdam, Netherlands: Elsevier Science Publishers; 1988. p. 95–108.
- Trapnell C, Adam R, Loyal G, et al. Differential gene and transcript expression analysis of RNA-seq experiments with TopHat and Cufflinks. *Nat Protoc*. 2012;7:562–78. <https://doi.org/10.1038/nprot.2012.016>.
- Tufail M, Naeemullah M, Elmogy M, et al. Molecular cloning, transcriptional regulation, and differential expression profiling of vitellogenin in two wing-morphs of the brown planthopper, *Nilaparvata lugens* Stål (Hemiptera: Delphacidae). *Insect Mol Biol*. 2010;19(6):787–98. <https://doi.org/10.1111/j.1365-2583.2010.01035.x>.
- Vellichirammal NN, Gupta P, Hall TA, et al. Ecdysone signaling underlies the pea aphid transgenerational wing polyphenism. *Proc Natl Acad Sci*. 2017;114(6):1419–23. <https://doi.org/10.1073/pnas.1617640114>.
- Villa F, Simon A, Ortiz BM, et al. Ctf4 is a Hub in the eukaryotic replisome that links multiple CIP-Box proteins to the CMG helicase. *Mol Cell*. 2016;63(3):385–96. <https://doi.org/10.1016/j.molcel.2016.06.009>.
- Wang XX, Zhang Y, Zhang ZF, et al. Deciphering the function of Octopamine-ergic signaling on wing polyphenism of the pea aphid *Acyrtosiphon pisum*. *Front Physiol*. 2016;7:603. <https://doi.org/10.3389/fphys.2016.00603>.
- Whitfield M, Thomas L, Bequignon E, et al. Mutations in *DNAH17*, encoding a sperm-specific axonemal outer dynein arm heavy chain, cause isolated male infertility due to asthenozoospermia. *Am J Human Genetics*. 2019;105(1):198–212. <https://doi.org/10.1016/j.ajhg.2019.04.015>.
- Willis KJ. State of the world's plants. London: Royal Botanic Gardens Kew; 2017.
- Xu HJ, Xue J, Lu B, et al. Two insulin receptors determine alternative wing morphs in planthoppers. *Nature*. 2015;519(7544):464. <https://doi.org/10.1038/nature14286>.
- Yoshida K, Kuo F, George EL, et al. Requirement of CDC45 for postimplantation mouse development. *Mol Cell Biol*. 2001;21:4598–603. <https://doi.org/10.1128/mcb.21.14.4598-4603.2001>.
- Zhang CX, Brisson JA, Xu HJ. Molecular mechanisms of wing polymorphism in insects. *Physiol Biochem Zool*. 2019;64:297–314. <https://doi.org/10.1146/annurev-ento-011118-112448>.
- Zhang TT, Liu NY, Wei W, et al. Integrated analysis of weighted gene co-expression network analysis identifying six genes as novel biomarkers for Alzheimer's disease. *Oxid Med Cell Longev*. 2021;2021:9918498. <https://doi.org/10.1155/2021/9918498>.
- Zhang S, Luo JY, Lv LM, et al. Effects of *Lysiphlebia japonica* (Ashmead) on cotton-melon aphid *Aphis gossypii* Glover lipid synthesis. *Insect Mol Biol*. 2015;24(3):348–57. <https://doi.org/10.1111/imb.12162>.
- Zhu CJ, Zhou ZC. Research progresses on the structure and function of KIF18A. *J Tianjin Normal Univ*. 2020;40:1–8.